MILLERITE AND OTHER NICKEL SULFIDES
FROM THE SIDERITE DEPOSIT
„STEIRISCHER ERZBERG", STYRIA, AUSTRIA

Eugen Libowitzky*[1], Anton Beran[1] & Richard Göd[2]

[1]Institut für Mineralogie und Kristallographie
[2] Department of Lithospheric Research
Universität Wien, Althanstrasse 14, 1090 Wien / *eugen.libowitzky@univie.ac.at

Abstract

Millerite, NiS, has been identified for the first time in cinnabar- and pyrite-bearing siderite ore samples from „Steirischer Erzberg", Styria, Austria. In addition, the occurrence of other nickel sulfides has been confirmed, such as siegenite-violarite solid-solutions (ss), $CoNi_2S_4$- $FeNi_2S_4$, and Gersdorffite, Ni[AsS]. Whereas millerite and gersdorffite are close to ideal chemistry with only minor Co and Fe contents, siegenite-violarite ss show a wide range of compositions. Almost pure siegenite with Fe below detection limit occurs in separated crystals within cinnabar or millerite. In contrast, small grains (sometimes in equilibrium with millerite) within a pyrite host contain up to ~14.1 wt% Fe and thus plot in the compositional field of violarite.

Zusammenfassung

Millerit, NiS, wurde zum ersten mal in Zinnober- und Pyrit-führenden Sideriterzproben vom Steirischen Erzberg, Steiermark, Österreich, nachgewiesen. Zusätzlich wurde auch das Vorkommen weitere Nickelsulfide wie Siegenit-Violarit-Mischkristalle (ss), $CoNi_2S_4$-$FeNi_2S_4$, und Gersdorffit, Ni[AsS], bestätigt. Während Millerit und Gersdorffit nahe der Idealchemie mit nur geringen Co- und Fe-Gehalten sind, zeigen Siegenit-Violarit ss einen weiten Zusammensetzungsbereich. Nahezu reiner Siegenit mit Fe unter der Nachweisgrenze kommt in separaten Kristallen innerhalb von Zinnober und Millerit vor. Im Gegensatz dazu enthalten kleine Einschlüsse (manchmal im Gleichgewicht mit Millerit) im Pyrit bis zu ~14.1 Gew.-% Fe und fallen damit in das Zusammensetzungsfeld von Violarit.

Introduction

Many siderite occurrences of various sizes can be found in the Greywacke Zone of the Eastern Alps. At present, only the „Steirischer Erzberg" deposit, situated near the village Eisenerz in the province of Styria, is in operation. The Austrian iron ore production of about two million t/a is exclusively mined from this location. The Paleozoic Greywacke Zone belongs to the Upper Austroalpine nappe system

ranging from Ordovician to Carboniferous, with rock series consisting mainly of carbonates, metapelites and porphyroids (SCHÖNLAUB, 1979). The siderite mineralization is restricted to the tectonically highest segment, the „Noric Nappe". The ore body is generally hosted by fine-grained limestones of Devonian age. Metasomatic-epigenetic structures are dominant, and usually coarse-grained siderite exhibits discordant contacts with the limestones. Late-stage mineralizations in all lithologies comprise intense chloritization, formation of quartz crystals, hematite, and sulfides such as pyrite, chalcopyrite, and cinnabar (POLGÁRI et al., 2010).

Samples and experimental methods

During a field trip to „Steirischer Erzberg" in spring 2017, one of us (R.G.) took numerous samples of an obviously cinnabar-bearing siderite rock. Samples of this type, even with spectacular, more than cm-sized, euhedral cinnabar crystals, have been described from a pocket in the late 1970ies (HUBER & HUBER, 1979). A tentatively cut and roughly polished specimen (Fig. 1) confirmed macroscopically the occurrence of cinnabar and pyrite in a fresh light-brownish siderite, but (under the microscope) indicated also the presence of some tiny grains of uncommon ore minerals. Therefore, two perfectly polished, one-inch microscope sections were prepared from the most promising regions for a detailed study (Fig. 2). These samples were investigated by three destruction-free methods.

Optical microscopy and micro-photography was performed with an OLYMPUS BX51 transmitted-/reflected-light microscope with 5x, 10x, 20x, 40x objectives and 10x eye pieces, a 100 W halogen lamp, and a 24 MP SONY A6000 system camera.

Figure 1. Two cut and polished samples of siderite ore (light-brownish) from „Steirischer Erzberg". The cinnabar- (red) and pyrite- (metallic grains) bearing zones contains the Ni-sulfides. Width of photograph: ~10 cm.
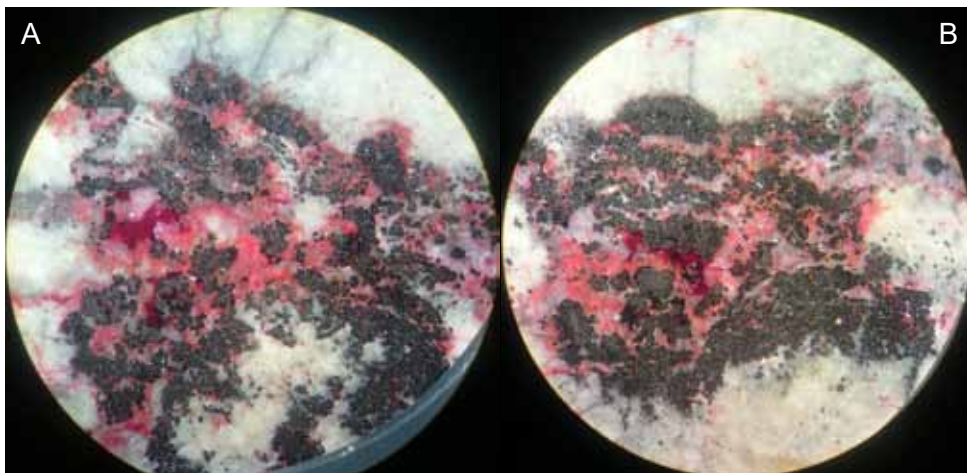
Figure 2. The two polished microscope sections viewed under a stereo microscope. Siderite appears creamy white, cinnabar is red, and pyrite grains show a dark metallic luster. Diameter of each field: ~2 cm.

Raman spectra were measured on a confocal micro-Raman spectrometer RENIS-HAW RM1000 equipped with a 20 mW Ar⁺ laser (blue, 488 nm) for excitation. A Leica DLML microscope with a 50x/0.75 objective, a 1200 lines/mm grating in a 300 mm monochromator, and a thermo-electrically cooled CCD detector were employed. The entrance slit and CCD readout were set to quasi-confocal mode. The resolution of the system (apparatus function) was ~5.5 cm⁻¹, and the Raman shift of the instrument was calibrated by the Rayleigh line and the 521 cm⁻¹ line of a Si standard. Spectra were acquired over 120 s, to obtain a good signal-to-noise ratio. Instrument set-up and control were done with Grams32 software, spectral analysis was performed with Peakfit4.12 (SeaSolve) and plotting with SigmaPlot9.01 (Systat).

Scanning electron microscopy (SEM) with energy-dispersive X-ray spectrometry (EDS) was conducted at a FEI InspectS SEM with an EDAX EDS system. The instrument was operated at an acceleration voltage of 15 kV, a spot size of 5.0, high vacuum conditions, and both secondary and backscatter electron detectors. X-ray spectra were acquired with an SDD Apollo XV X-ray detector and analyzed with EDAX Genesis software using internal standards. Detection limits are roughly at ~0.8-1.0 wt-%. Analytical errors are ~2% relative for main components, and up to ~10% for minor constituents.

Results and Discussion

Figures 3, 4a, and 5 show reflected light micrographs of the six sulfide ore minerals. The predominant phase is pyrite, FeS_2, in euhedral, subhedral and anhedral grains, abundantly sputtered with numerous inclusions, and sometimes with a skeletal appearance (Fig. 4). Quantitative EDS micro analyses at the SEM confirm the stoichiometric formula; in many cases X-ray spectra do not show any other element peaks, i.e., they are below detection limit (bdl). Only in a few cases Ni and Co were measured with up to ~2 wt%, resulting in a formula such as $(Fe_{0.93}Co_{0.03}Ni_{0.03})S_{2.01}$.
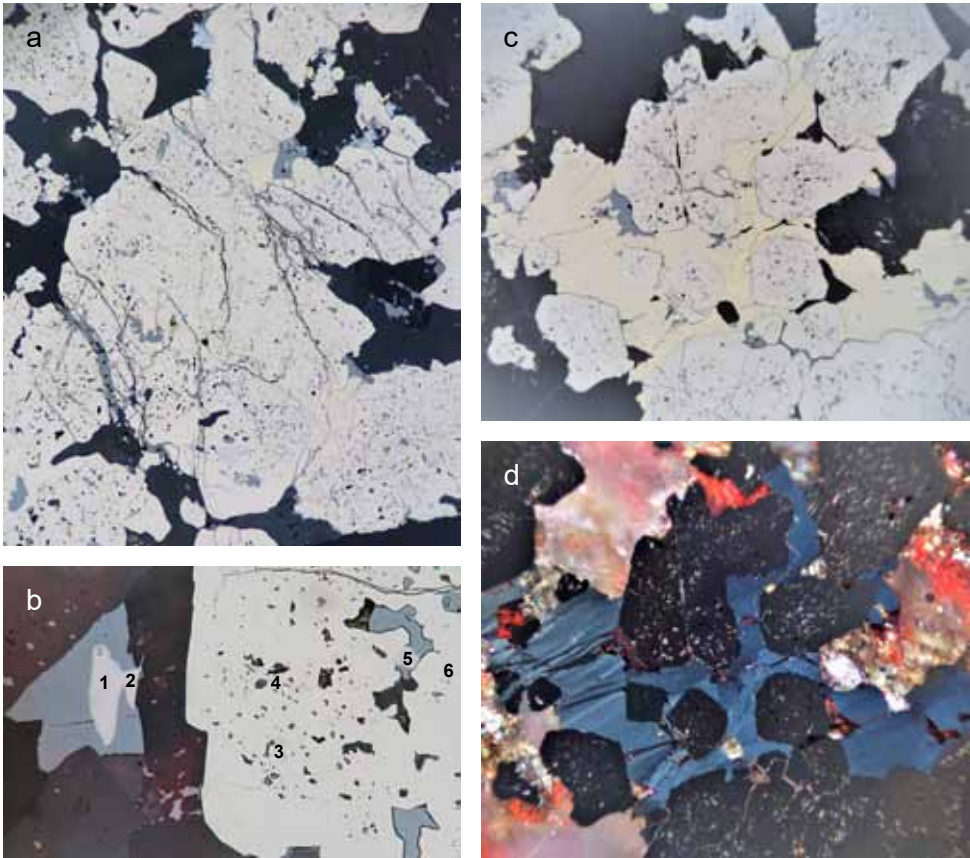
Figure 3. Reflected light photo micrographs. a) Overview containing all six sulfide ore minerals: predominantly pyrite (yellowish white), cinnabar (dark grey), gersdorffite (white), millerite (bright yellow), tiny chalcopyrite grains (dark yellow), siegenite-violarite ss (light grey with brownish tint), 600 μm width. b) Siegenite-violarite ss grains in cinnabar and pyrite, 250 μm width. Numbers refer to analysis spots of Table 1. c) Subhedral pyrite grains in a matrix of millerite and minor cinnabar, 750 μm width. d) Same as before with crossed polarizers. Pyrite is black, cinnabar shows red internal reflections, and millerite has intense blue anisotropy colors.

However, it cannot be ruled out that these analyses are biased by invisible submicron sized inclusions of Ni-Co-sulfides (see below) in pyrite.

In addition, the sections contain cinnabar, HgS, sometimes concentrated in the form of 2-3 mm large anhedral masses, or finely dispersed in tiny grains across the sections. It occurs also in numerous inclusions within pyrite. In a number of cases it appears to fill voids with sharp and rectangular border lines, e.g. Figs. 3b, 5a,c, resembling at least partially the form of cubes. The EDS spectra are free from impurity elements above detection limit.

The other four phases either are connected with cinnabar, or they occur in the form of tiny inclusions within pyrite in the cinnabar-rich zones. The least abundant and spectacular phase is chalcopyrite, $CuFeS_2$, which is present only in < 10 μm small anhedral grains (only one spot with ~100 μm size was observed). The EDS spectra
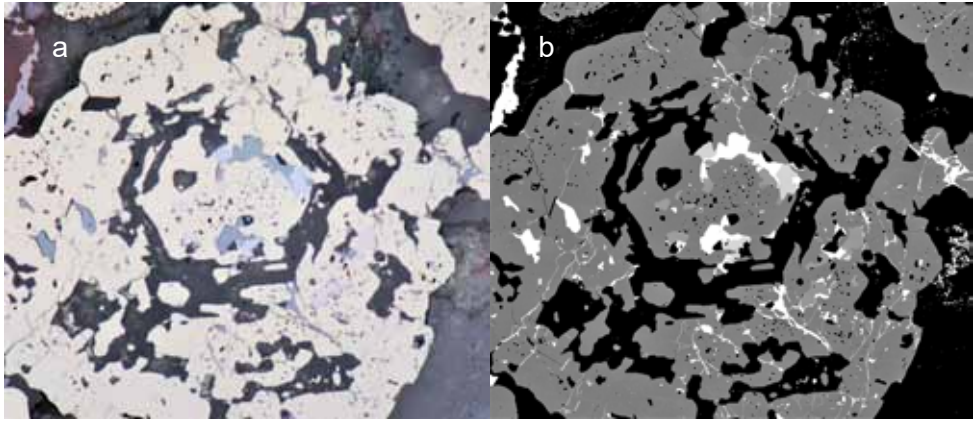
Figure 4. Skeletal dodecahedral pyrite crystal with numerous inclusions of cinnabar, gersdorffite, siegenite-violarite ss, and tiny chalcopyrite; 350 µm width. a) Reflected light photomicrograph. b) Electron backscatter image from the SEM (white=cinnabar, light grey=gersdorffite, medium grey=siegenite-violarite, dark grey=pyrite host).

commonly confirm its pure stoichiometry, e.g. $Cu_{0.99}Fe_{0.98}S_{1.03}$. Results with up to 2 wt% Ni, e.g., the spot from Fig. 5c, are obviously biased by interference with surrounding or at least neighboring Ni-sulfides. These nickel sulfides are the topic of this paper and are presented in detail below.
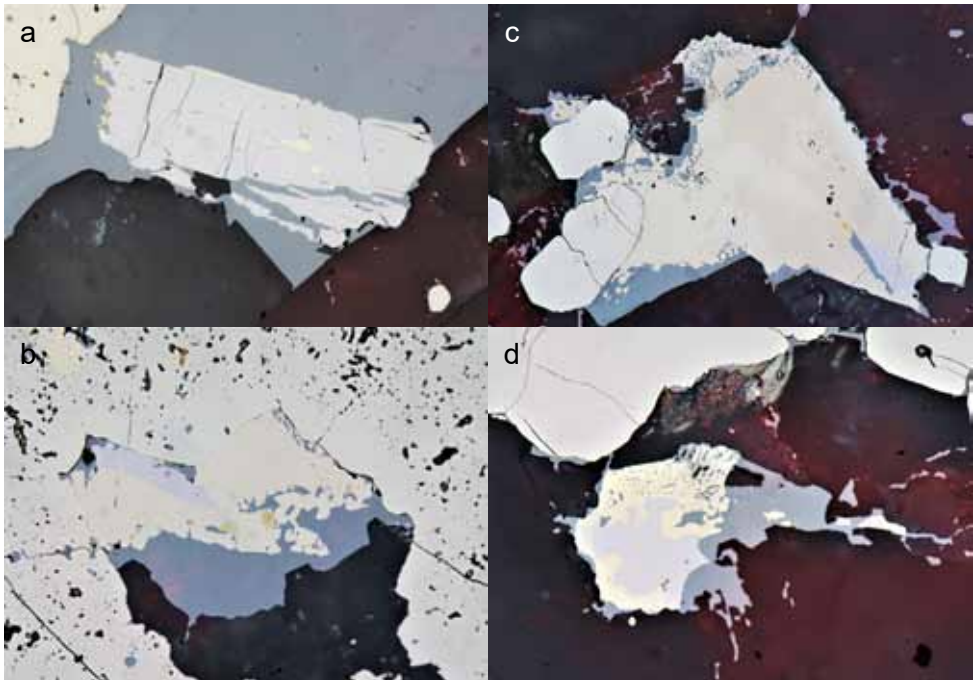

Figure 5. Reflected light micrographs of intergrowths of millerite, siegenite ss, and cinnabar (± tiny chalcopyrite). Widths of images are a) 250, b) 200, c) 300, and d) 200 µm.

Millerite

According to the authors' best knowledge, this is the first identification and description of millerite, NiS, from „Steirischer Erzberg", Styria, Austria. Using a reflected light microscope, it is easily recognized (MÜCKE, 1989) by its bright yellow color (similar reflectance as pyrite but more intense yellow; brighter than chalcopyrite – CRIDDLE, 1993) and the intense anisotropy colors under crossed polarizers from slate brown to grey-blue (Fig. 3d). Twin lamellae are common. Though needle-shaped crystals are characteristic, millerite occurs in the present samples with irregular shape, either in larger areas together with cinnabar as, e.g., in Fig. 3c (embedding pyrite crystals), or in the form of tiny inclusions in pyrite, e.g., upper left corner of Fig. 5b.

Micro-Raman spectra of millerite from „Steirischer Erzberg" are presented in Fig. 6 and compared to those of the mineral Raman database of the University of Mainz, Germany (L. Nasdala, pers. comm.). Three millerite spectra from the web-based RRUFF database (DOWNS, 2006) also confirmed our own results but were of rather poor quality. An accurate peak fit of the spectra resulted in excellent agreement of Raman band positions with those of a single-crystal study of millerite by GUILLAUME et al. (2008) (values in parentheses): 149 (149), 231 (230), 250 (250), 303 (300), 353 (352), 374 (373) cm^{-1}. However, it should be noted that the accurate Raman peak positions may depend on the preparation procedure of the polished sections (LIBOWITZKY et al., 2006).

A total of 61 EDS microanalyses of millerite have been performed. Data are summarized in Table 1, and the (rather narrow) range of compositions is depicted in Figure 7. In general there are numerous analyses that are very close to the ideal
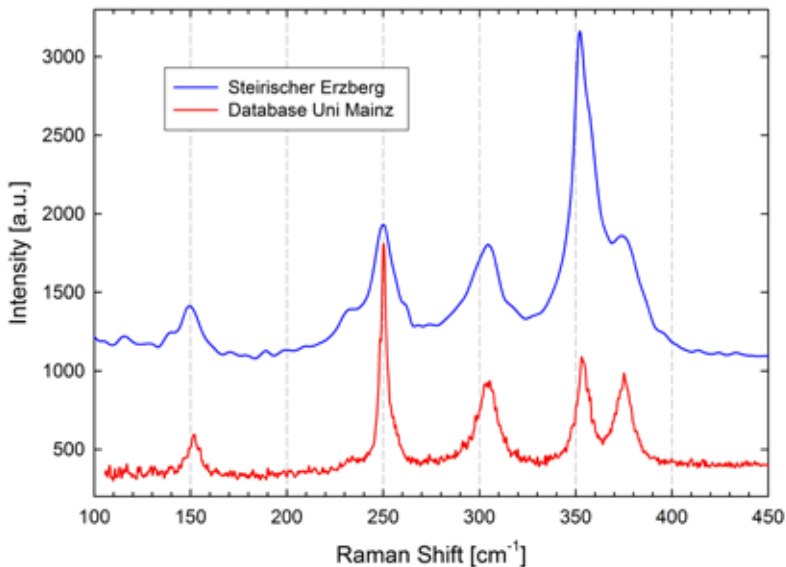

Figure 6. Raman spectra of millerite from the „Steirischer Erzberg" and from the mineral Raman database of the University of Mainz, Germany (L. Nasdala, pers. comm.).

Table 1: EDS microanalyses of Ni-sulfides in wt% and atoms per formula unit (apfu).

[wt%]	Millerite[*] mean (range), n=51	Siegenite-ss low-Fe #1 #2 #5			Siegenite-ss high-Fe #3 #4 #6			Gersdorffite mean (range), n = 13
Ni	64.33 (61.93-65.93)	41.16	40.70	41.13	37.17	37.43	37.10	31.24 (29.95-32.56)
Co	bdl (bdl - 1.91)	16.72	17.62	15.45	10.04	10.71	10.18	0.83 (bdl - 1.69)
Fe	bdl (bdl - 1.58)	0.47[§]	0.78[§]	1.86	10.55[$]	9.65	10.84[$]	1.65 (bdl - 2.69)
As	-	-	-	-	-	-	-	46.35 (45.76-47.11)
Sb	-	-	-	-	-	-	-	2.42 (1.53-3.63)
S	35.33 (33.85-36.46)	41.66	40.90	41.55	42.24	42.20	41.88	17.50 (17.12-17.86)
[apfu]	(<u>Ni</u>,Co,Fe)S	(<u>Ni</u>,<u>Co</u>,Fe)$_3$S$_4$			(Ni,Co,Fe)$_3$S$_4$			(<u>Ni</u>,Co,Fe)[(<u>As</u>,Sb)S]
Ni	0.99 (0.96-1.03)	2.14	2.13	2.14	1.92	1.93	1.92	0.91 (0.87-0.94)
Co	bdl (bdl - 0.03)	0.87	0.92	0.80	0.52	0.55	0.53	0.02 (bdl - 0.05)
Fe	bdl (bdl - 0.03)	0.03	0.04	0.10	0.57[$]	0.52	0.59[$]	0.05 (0.03-0.08)
As	-	-	-	-	-	-	-	1.05 (1.04-1.07)
Sb	-	-	-	-	-	-	-	0.03 (0.02-0.05)
S	1.00 (0.97-1.03)	3.97	3.91	3.96	3.99	3.99	3.97	0.93 (0.91-0.95)

<u>*Notes:*</u> *Analysis spots #1 - #6 refer to those in Fig. 3b. bdl = below detection limit. [*] Only unbiased analyses – see also text and Fig. 8. [§] Actually below detection limits – the analytical error exceeds the value. [$]With Fe > Co these ss members actually belong to violarite.*

stoichiometric composition NiS with Ni and Co below or close to detection limits. The maximum Co contents are ~2 wt% (~0.03 apfu). In contrast, the Fe values apparently reach 14 wt% (~0.22 apfu). However, as Fig. 7 shows, these high Fe contents correlate well with excess sulfur concentrations of up to ~1.09 apfu. In fact, these data may be biased, i.e., they contain „mixed analyses" that can be deconvoluted into a pyrite contribution plus the millerite data. This observation is supported by the fact that all 10 high-Fe analyses are exclusively from tiny millerite inclusions in pyrite. Thus, data in Table 1 have been constrained to 51 unbiased data sets. Nevertheless, there exist data with elevated iron contents and S values of 0.98-1.01 S apfu. These will be discussed below.

Siegenite-Violarite solid-solutions

Under the reflected light microscope, the most characteristic features of the sulfide spinel siegenite, are its creamy gray color with a brownish-pink hue (MÜCKE, 1989), and its optically isotropic behavior (cubic symmetry). In the samples from „Steirischer Erzberg" it occurs either in contact with cinnabar in the form of up to ~200 μm large subhedral grains (Fig. 5a) and as round to elongated grains in or
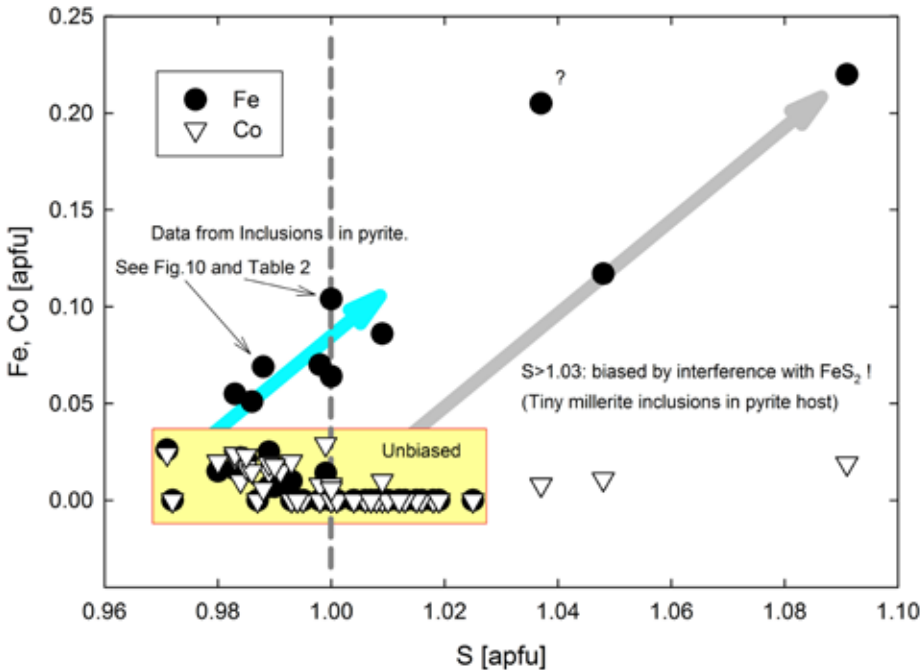
Figure 7. Fe and Co contents versus S (as an indicator for stoichiometry) from EDS microanalyses of millerites from the „Steirischer Erzberg". The correlation of high Fe with excess S values (gray arrow) indicates biased analyses, i.e. mixed analyses from tiny millerite inclusions in a pyrite host. The elevated Fe contents at normal stoichiometry (0.98 < S < 1.01, blue arrow) appear to be correct, though also from pyrite inclusions.
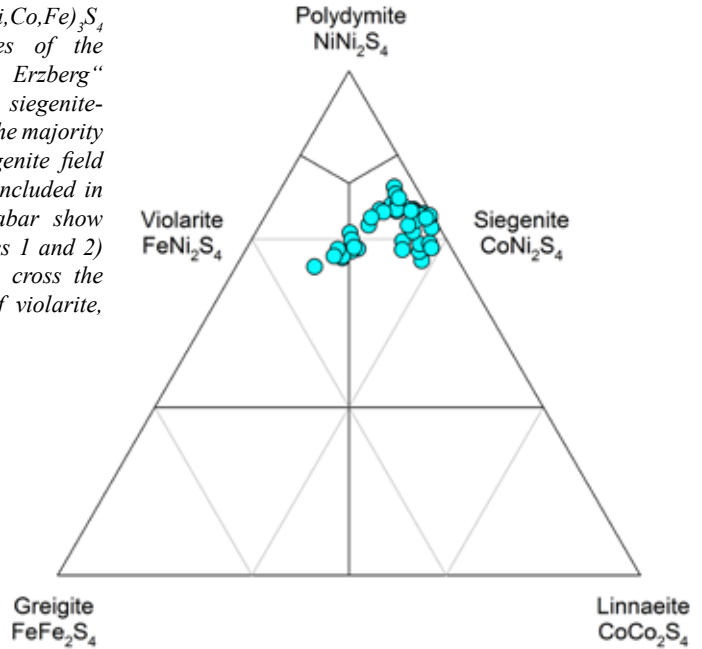
close to millerite (Figs. 5b,c), or in the form of tiny inclusions (also in equilibrium with millerite – see below) within pyrite.

EDS microanalyses show a considerably variable composition of this Ni sulfide (Fig.8, examples in Table 1). A chemistry close to siegenite, $CoNi_2S_4$, is confirmed in the larger grains, which are surrounded by cinnabar and not in contact to pyrite, e.g. the left grain in Fig. 3b, and the core in Fig.5d). In these samples, the Ni content is elevated (~2.1-2.2 apfu) and Fe remains below or close to the detection limit („low-Fe" in Table 1). In contrast, samples without cinnabar and in direct contact with pyrite, especially the tiny inclusions in pyrite, may contain up to ~14.1 wt% Fe and thus touch or even cross (if Fe > Co) the borderline towards violarite, $FeNi_2S_4$ („high-Fe" in Table 1 and inclusions in Table 2). Between these extremes, numerous compositions have been observed and plotted in Fig. 8. However, the six analysis spots in Figure 3b and Table 1, which are in close neighborhood, show these contrasting compositions most convincingly. The most Fe-rich siegenite-violarite ss are from inclusions in equilibrium with millerite and are discussed below.

Gersdorffite

The only sulfarsenide of the present samples is gersdorffite, Ni[AsS]. The white and optically isotropic anhedral grains (MÜCKE, 1989) are rarely found in only

Figure 8. Ternary plot of (Ni,Co,Fe)$_3$S$_4$ spinels. EDS microanalyses of the samples from „Steirischer Erzberg" confirm the occurrence of siegenite-violarite ss, ~(Co,Fe)Ni$_2$S$_4$. The majority of analyses plot in the siegenite field ~CoNi$_2$S$_4$. However, grains included in pyrite without visible cinnabar show rather high Fe values (Tables 1 and 2) and, in a number of cases, cross the border line into the field of violarite, ~FeNi$_2$S$_4$.

limited areas, mostly at the rims of larger pyrite masses (Fig. 3a) or included within the skeletal pyrite crystal in Fig. 4. It is always in contact to cinnabar.

A total of 13 EDS analyses show a very narrow chemistry of gersdorffite from „Steirischer Erzberg". Similar to millerite the substitution of Ni by Co and Fe is clo-

Table 2: EDS microanalyses of Ni-sulfide inclusions in pyrite (see Fig. 10).

[wt%]	Siegenite-ss1	Millerite1	Siegenite-ss2	Millerite2	Pyrite
Ni	35.90	57.77	37.29	60.53	1.09
Co	7.98	0.41*	9.37	0.40*	1.61
Fe	14.13§	6.40	11.72§	4.23	43.63
S	41.99	35.42	41.62	34.84	53.67
[apfu]	(Ni,Co,Fe)$_3$S$_4$	(<u>Ni</u>,Co,Fe)S	(Ni,Co,Fe)$_3$S$_4$	(<u>Ni</u>,Co,Fe)S	(Ni,Co,<u>Fe</u>)S$_2$
Ni	1.85	0.89	1.93	0.94	0.02
Co	0.41	<0.01*	0.48	<0.01*	0.03
Fe	0.77§	0.10	0.64§	0.07	0.94
S	3.97	1.00	3.95	0.99	2.01

<u>Notes:</u> * Actually below detection limits – the analytical error exceeds the value.
§With Fe > Co these members of the siegenite-violaritede ss definitely belong to violarite.
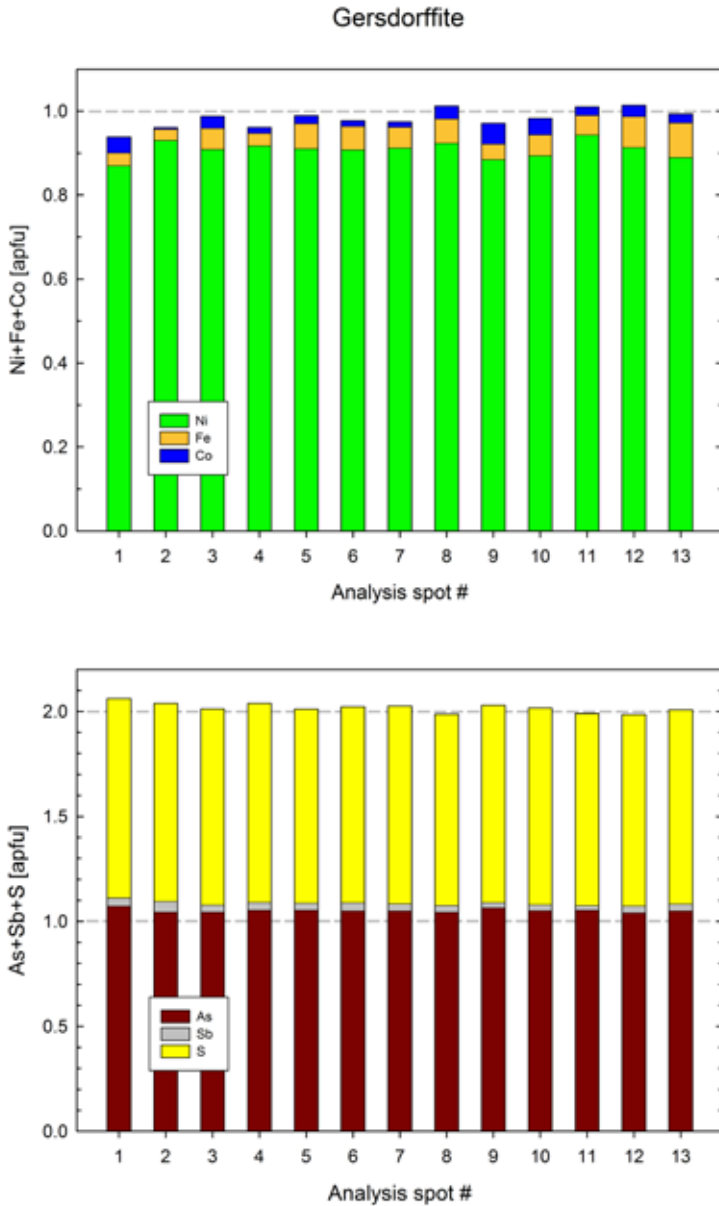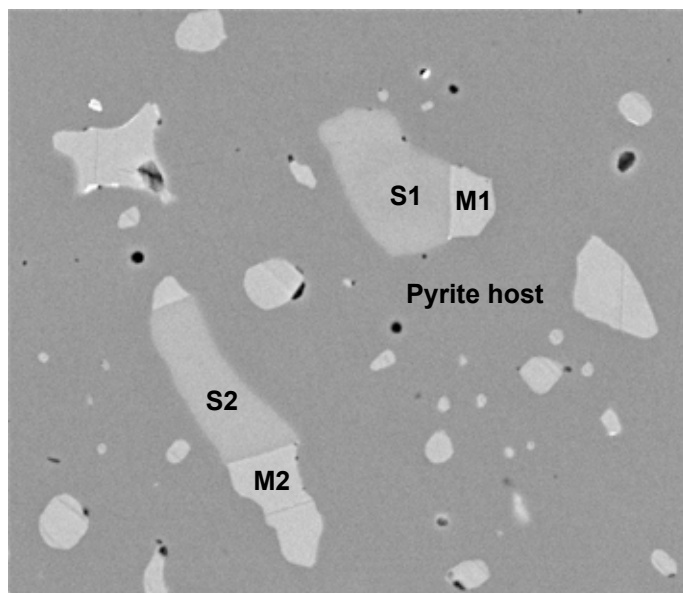
Figure 9. Analyses of gersdorffite from „Steirischer Erzberg", indicating the rather constant composition across the sample section. Upper plot: occupancy of the metal position. Lower plot: composition of the anion group.

se to or slightly above detection limits, i.e., on average 0.83 wt% Co and 1.65 wt-% Fe (Table 1, Fig. 9). The sulfarsenide anion group reveals constantly elevated As contents with minor Sb substitution, and is slightly depleted in sulfur (Table 1, Fig. 9). The resulting mean formula of gersdorffite is $(Ni_{0.91}Co_{0.02}Fe_{0.05})_{\Sigma=0.98}[(As_{1.05}Sb_{0.03})_{\Sigma=1.08}S_{0.93}]_{\Sigma=2.01}$.

Figure 10. Electron back-scatter image of inclusions in pyrite. Width of image is 25 μm. S1,S2 = siegenite-violarite ss, M1,M2 = millerite, see Table 2.

Mineral relations/reactions and genetic considerations

Figures 1 and 2 show very fine gray fissures that end up in the pyrite-cinnabar-bearing zones. Thus, the described ore mineral assemblage has been formed epigenetically in a late stage after the crystallization of siderite and ankerite, which are the primary economic ores at „Steirischer Erzberg". The occurrence of the Ni sulfides and cinnabar as inclusions within pyrite (Fig. 3a), the skeletal growth of pyrite (Fig. 4), as well as the occurrence of pyrite and siegenite-violarite ss within millerite (Figs. 3c,d), suggest a fast and simultaneous crystallization of these ore minerals. In a number of cases, the filled pyrites show a final solid growth zone without any inclusions at the rim.

Close-up reflected-light microphotographs in Fig. 5, especially the remarkable core-rim structure in Fig. 5d may indicate that siegenite (remaining in the core with Fe = bdl) has been consumed by cinnabar with simultaneous eutectoidal crystallization and intergrowth of cinnabar and millerite. These eutectoidal structures of HgS and NiS and a relictic siegenite lamella are observed also in the close-ups in Figs. 5b and c. And even in Fig. 5a a fine rim of millerite is revealed at the border of siegenite towards cinnabar. Copper is limited to the tiny chalcopyrite grains, e.g. in Figs. 5a-c; the Ni phases do not contain copper contents above detection limits.

An electron backscatter image of the fine inclusions in a pyrite grain shows two spots with siegenite-violarite ss in equilibrium (at a straight grain boundary) with millerite within ~5 μm wide inclusions. Table 2 shows the EDS analyses of these spots. It is remarkable that the compositions of the siegenite-violarite ss are the most Fe-rich of all, and clearly fall in the field of violarite (the lower-left two data points in Fig. 8). The millerites show elevated Fe contents of up to 6.4 wt%. However, the correct stoichiometry with S ~1.00 indicates that these analyses are not biased by interference with the surrounding pyrite (see discussion of millerite above). The host pyrite reveals low Co and Ni contents that are close to or slightly

above detection limits (Table 2). However, these values may result from invisible, submicroscopic inclusions of the described Co-Ni-sulfide phases within pyrite.

In general, the element distribution in the observed nickel sulfides clearly indicates that only the sulfide spinel structure of siegenite-violarite ss is susceptible to the incorporation of cobalt in its tetrahedrally coordinated $Me^{[4]}$ sites within the cubic close packing of sulfur atoms. In contrast, the octahedrally coordinated $Me^{[6]}$ sites in pyrite or gersdorffite, and the square pyramidal coordination of $Me^{[4+1]}$ in millerite (STRUNZ & NICKEL, 2001) are comparably less attractive.

References

CRIDDLE, A. (1993): The quantitative data file for ore minerals, 3rd Ed. - Chapmann & Hall, London.

DOWNS, R.T. (2006): The RRUFF Project: an integrated study of the chemistry, crystallography, Raman and infrared spectroscopy of minerals. – Progr. Abstr. 19th General Meeting IMA, Kobe, Japan. O03-13.

GUILLAUME, F., HUANG, S, HARRIS, K. D. M., COUZI, M. & TALAGA, D. (2008): Optical phonons in millerite (NiS) from single-crystal polarized Raman spectroscopy. – J. Raman Spectr. 39, 1419-1422.

HUBER, S. & HUBER, P. (1979): Neue Zinnoberfunde vom Steirischen Erzberg. - Lapis 4, 66.

LIBOWITZKY, E., BECHTOLD, A., FRIESL, P., OBERWANDLING, L. & WILDNER, M. (2011): Influence of surface defects on Raman spectra of ore minerals. - 7th ECMS Abstr. Vol., 44.

MÜCKE, A. (1989): Anleitung zur Erzmikroskopie: mit einer Einführung in die Erzpetrographie. - Enke, Stuttgart.

POLGÁRI, M., PROCHASKA, W. & BERAN, A. (2010): Alpine carbonate mining sites: Aspects of carbonate mineralizations related to the manganese mine of Úrkút, Hungary, the magnesite deposit of Veitsch and the siderite mine "Steirischer Erzberg", Austria. - Acta Miner. Petrogr., Field Guide Series 4, 1-16.

SCHÖNLAUB, H. P. (1979): Das Paläozoikum in Österreich. – Abh. Geol. Bundesanst. 33, 3-124.

STRUNZ, H. & NICKEL, E. H. (2001): Strunz Mineralogical Tables. Chemical-Structural Mineral Classification System, 9th Ed. - Schweizerbart, Stuttgart.